Bandwidth control of the spin diffusion through interfaces and the electron-phonon coupling in magnetoresistive manganites

J. Fontcuberta, B. Martínez, V. Laukhin, Ll. Balcells, X. Obradors, C. H. Cohenca and R. F. Jardim

Phil. Trans. R. Soc. Lond. A 1998 **356**, 1577-1591
doi: 10.1098/rsta.1998.0236

Bandwidth control of the spin diffusion through interfaces and the electron–phonon coupling in magnetoresistive manganites

By J. Fontcuberta[1], B. Martínez[1], V. Laukhin[1]†, Ll. Balcells[1],
X. Obradors[1], C. H. Cohenca[2] and R. F. Jardim[2]

[1]*ICMAB-CSIC, Campus Universitat Autònoma de Barcelona,*
E-08193 Bellaterra, Spain
[2]*Instituto de Fisica, Universidade de Sao Paulo, 05315-970 Sao Paulo, Brazil*

Electronic bandwidth in ferromagnetic manganese perovskites is known to control several significant properties. In this paper we take advantage of this remarkable property to show that the interface scattering, leading to low-field magnetoresistivity (LFMR), and electron–phonon coupling can be modified by using the appropriate chemical substitutions. The magnetoresistance and the magnetization of ceramic $\mathrm{L}_{2/3-x}\mathrm{L}'_x\mathrm{A}_{1/3}\mathrm{MnO}_3$ (L,L$'$ = lanthanides, A = Sr, Ca) oxides have been studied as a function of the grain size. It is found that these ceramics become magnetically harder when reducing the particle size and display a gradual increase in low-field magnetoresistance. Narrowing the bandwidth reinforces these effects. We suggest that both phenomena could be closely related and associated with the existence of some degree of spin disorder at the grain boundaries.

On the other hand, the dependence of the Curie temperature on hydrostatic pressure P for several samples have been determined. It is found that the Curie temperature, T_{C}, being itself a function of the electronic bandwidth W, displays a larger variation of $\mathrm{d}\ln T_{\mathrm{C}}/\mathrm{d}P$ as the bandwidth is reduced. However, the observed $\mathrm{d}\ln T_{\mathrm{C}}/\mathrm{d}P$ versus T_{C} or W variations are found to be significantly larger than expected on the basis of simple steric modifications of bandwidth. We suggest that the electron–phonon coupling is substantially reduced under pressure, this effect being more prominent as the bandwidth is reduced.

Keywords: magnetoresistance; perovskites; pressure; electron–phonon coupling; interfaces

1. Introduction

The colossal magnetoresistance (MR) of manganese perovskites (up to 10^7% (Jin *et al*. 1994)) has a serious drawback on the need for large magnetic fields to obtain such large changes of resistance. This fact is an important handicap since many of their potential applications require a good response in the low-field regime. In this sense, the discovery of two well-separated MR contributions in ceramic $\mathrm{La}_{2/3}\mathrm{A}_{1/3}\mathrm{MnO}_3$ (A = Ca, Sr) samples, one attributed to an intrinsic intragranular component and the other to a non-intrinsic intergranular effects (Hwang *et al*. 1996), could be of a major importance for technological applications.

---

† Permanent affiliation: Institute of Chemical Physics in Chernogolovka, Russia.

Phil. Trans. R. Soc. Lond. A (1998) **356**, 1577–1591
Printed in Great Britain

TEX Paper

Although the actual mechanism behind the low-field magnetoresistive response (LFMR) is still obscure, spin-polarized intergrain tunnelling through interfaces (Hwang *et al*. 1996) and spin-dependent scattering at the grain boundaries (Li *et al*. 1997) have been proposed. It is therefore evident that, whatever the mechanism, a strong influence of the surface magnetic disorder on the conduction process should be expected. Therefore, reducing the particle size of the ceramics would imply an increase in the number of junctions and the LFMR should be significantly enhanced.

On the other hand, according to the current understanding of the spin-tunnelling mechanism, the LFMR should be proportional to the intergrain-exchange coupling (Helman & Abeles 1976), which can be tuned by appropriate tailoring of both bulk and surface magnetic interactions (García-Muñoz *et al*. 1997; Fontcuberta *et al*. 1996*a*, *b*; Hwang *et al*. 1995*a*; Tokura *et al*. 1996). It has been shown that the degree of spin disorder can be controlled via the $\sigma^{1-x}(e_g)$ bandwidth, by the appropriate choice of lanthanide (Fontcuberta *et al*. 1996*a*). At the grain surface of a ceramic sample, charge-carrier mobility should be severely dampened, the relative strength of the ferromagnetic F to antiferromagnetic AF interactions F/AF reduced and, therefore, their competition reinforced. At the same time, charge carriers in manganites are fully polarized and in a transport experiment, a current of carriers should travel from grain to grain. Thus, surface spin disorder should severely affect the intergrain resistivity, in a very sensitive way. In this paper we will explore the influence of both particle size and magnetic disorder on the low-field magnetoresistive response of ceramic manganites. To that purpose ceramic samples of varying particle size and having progressively narrower bandwidths (i.e. weaker ferromagnetic interactions) will be prepared and their magnetotransport properties investigated. It turns out that for a given bandwidth W, when increasing the particle size the LFMR is significantly reduced. Alternatively, while keeping the particle size constant, when reducing W, the LFMR increases and clear signatures of a magnetically disordered interface can be inferred from experiments (Fontcuberta *et al*. 1998).

In double-exchange (DE) ferromagnetic perovskites, high pressure increases the relevant Mn–O–Mn orbital overlapping (t_{ij}), thus leading to a broader bandwidth W for the itinerant e_g electrons. As a consequence, the ferromagnetic coupling increases and the Curie temperature, T_{C}, where an insulator–metal transition is commonly observed, rises. The bandwidth is controlled by both the Mn–O distance ($d_{\mathrm{Mn-O}}$) and the bending angle, Θ, of the Mn–O–Mn bond.

Internal pressure can be achieved by partial substitution of the lanthanide by other cations of larger ionic radii. By using this approach it has been shown that T_{C} can be conveniently tuned: when reducing the mean ionic size (R_{o}) of the lanthanide, T_{C} gradually lowers (Fontcuberta *et al*. 1996*a*, *b*; Hwang *et al*. 1995*a*; Tokura *et al*. 1996). Extensive structural analysis showed that the relevant change is the bond angle Θ which closes as R_{o} is reduced, whereas $d_{\mathrm{Mn-O}}$ does not change appreciably (García-Muñoz *et al*. 1997). Consequently, in chemically induced pressure experiments, band broadening and thus T_{C} is mainly controlled by the stretching of the Mn–O–Mn bond.

Application of external pressure (P) can modify both $d_{\mathrm{Mn-O}}$ and Θ. In fact, in the closely related $\mathrm{LNiO_3}$ perovskites, it has been shown that $d_{\mathrm{Ni-O}}$ compresses under pressure, whereas Θ opens ($\partial d_{\mathrm{Ni-O}}/\partial P < 0$ and $\partial\Theta/\partial P > 0$ (Medarde *et al*. 1995); thus both variations add to increase the effective bandwidth W. Very recent experiments on $\mathrm{L_{2/3}A_{1/3}MnO_3}$ have also found similar effects (Radaelli *et al*. 1997).

Therefore, experiments under hydrostatic pressure should lead to *positive* $\mathrm{d}T_{\mathrm{C}}/\mathrm{d}P$, reflecting the $d_{\text{Mn–O}}$ and Θ contributions to $\mathrm{d}W/\mathrm{d}P$.

In this paper we will also report on pressure effects on a series of $\mathrm{L}_{2/3}\mathrm{A}_{1/3}\mathrm{MnO}_3$ ceramic perovskites having a wide range of variation in the mean radius R_{o}. This enables us to study the dependence of $\mathrm{d}T_{\mathrm{C}}/\mathrm{d}P$ on the itinerant carrier bandwidth $W(d_{\text{Mn–O}}, \Theta)$. Two results will emerge from this study. First, the different sensitivity to pressure along the series mainly results from the difference in Θ, bond length compressibility only having a secondary role. Second, and more relevant, is the fact that according to the current understanding of the $W(d_{\text{Mn–O}}, \Theta)$ bandwidth dependence of T_{C} and the data for compressibilities $\kappa(\alpha)$ ($\kappa(\alpha) = (1/\alpha)(\partial\alpha/\partial P)$, where α stands for the Mn–O bond length ($d_{\text{Mn–O}}$) or Mn–O–Mn angle (Θ)), the evaluated dependence of $\mathrm{d}\ln T_{\mathrm{C}}/\mathrm{d}P$ on T_{C} (or W) is much weaker than observed. As a consequence, for the narrowest band materials, $\mathrm{d}\ln T_{\mathrm{C}}/\mathrm{d}P$ is predicted to be almost one order of magnitude smaller than measured. In order to account for such a discrepancy the precise nature of carriers should be included in the analysis. Our findings indicate that the coupling between the free carriers and the phonon lattice is also modified by internal or external pressure (Laukhin *et al*. 1997).

(*a*) *Experimental*

Most of the $(\mathrm{L,L'})_{2/3}\mathrm{A}_{1/3}\mathrm{MnO}_3$ (L,L′ = Nd, La, Sm; A = Ca, Sr) ceramics were prepared by conventional solid-state techniques and samples sintered in an oxygen atmosphere (García-Muñoz *et al*. 1997; Fontcuberta *et al*. 1996*a*); the $\mathrm{La}_{2/3-x}\mathrm{Y}_x\mathrm{Ca}_{1/3}\mathrm{MnO}_3$ ($x = 0$–0.25) samples used in the study of bandwidth effects on LFMR were prepared by a sol-gel method (Fontcuberta *et al*. 1998; Suzuki & Jardim 1996). The particle size effects were studied in a series of four samples (A–D) of $\mathrm{La}_{2/3}\mathrm{Sr}_{1/3}\mathrm{MnO}_3$ with particle sizes of 0.5–1 µm (A), 2–5 µm (B), 10–20 µm (C) and 50–100 µm (D) prepared by using different methods (mechanical attrition and different sintering temperatures) in order to control particle size (Balcells *et al*. 1998). Bandwidth effects were explored in a series of $\mathrm{La}_{2/3-x}\mathrm{Y}_x\mathrm{Ca}_{1/3}\mathrm{MnO}_3$ ($x = 0$–0.25) samples. Magnetization measurements were made by using a QD SQUID system up to 5 T. Transport measurements were made by using the standard four-probe method, on samples of about $0.5 \times 1 \times 5\ \mathrm{mm}^{-3}$ with the current applied perpendicular to the magnetic field.

A quasi-hydrostatic pressure was obtained by using a clamp-type piston cylinder cell with silicon organic liquid as a pressure-transmitting medium (Laukhin *et al*. 1997).

2. Magnetoresistance at interfaces

In figure 1 we show the $\rho(T)$ curves for samples A–D. The electrical resistivity has essentially the very same form and steadily increases, throughout the temperature range, from sample D to sample A, reflecting the grain size reduction. An apparent maximum of resistivity exists at $T \approx 365$ K for all the samples, thus showing that the oxygen stoichiometry is essentially the same. Magnetization measurements (not shown) revealed coincident Curie temperatures and identical (within the experimental error) saturation magnetization.

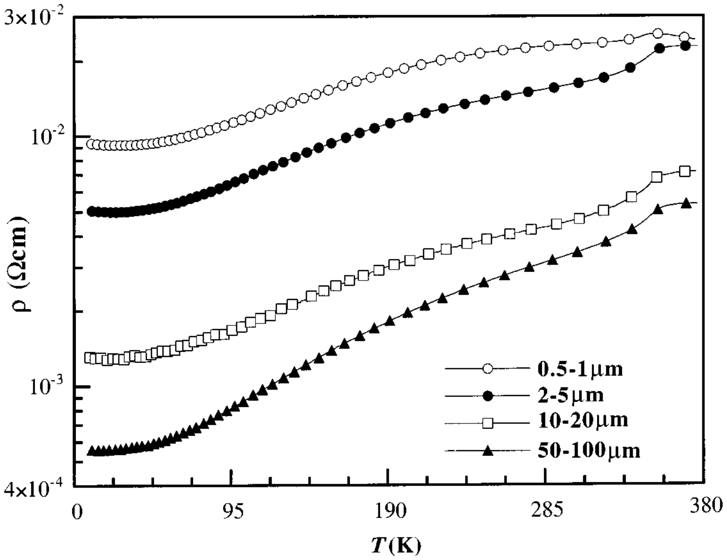

Figure 1. Thermal dependence of the electrical resistivity of the $La_{2/3}Sr_{1/3}MnO_3$ samples as a function of the particle size.

As already observed in ceramic samples of the same composition (Hwang *et al.* 1996), the magnetoresistance (MR) of samples A–D, as a function of field, displays two well-defined regimes (Balcells *et al.* 1998). In the low-field regime extending only a few kOe, a sharp decrease is found, with variations of MR up to 30% at low temperatures, but decreasing when T increases. On the contrary, in the high field regime the variation of MR is almost linear with a slope $S = \mathrm{d}R(H)/\mathrm{d}H$ very much smaller than for low fields.

The low-field MR may be evaluated by extrapolating back to $H = 0$, the almost linear behaviour of the normalized resistance $(R(H)/R(0))$ observed above 5 kOe. Subtracting the intercept with the Y-axis from 1 we have the variation of the MR in the low-field regime, the so-called low-field magnetoresistance (LFMR) depicted in figure 2. The key point in this figure is that LFMR not only decreases with T, but also clearly depends on the particle size, becoming smaller as the particle size increases. It is also worth mentioning that the MR does not show the expected quadratic dependence on the magnetization at any temperature (see inset of figure 2). Although one should note that if the magnetoresistance is strongly related to interface magnetism, it should influence the measured resistivity but not the overall magnetization (M), which is essentially a bulk measurement.

A key issue in the data of figure 2 is the temperature dependence of the LFMR, which displays a functional form akin to the Curie–Weiss-law, i.e. $\mathrm{LFMR}(T) = \alpha + \beta/(T+\theta)$. The solid lines through the data in figure 2 are the fits to this expression. It turns out that the fitting parameter, θ, increases monotonously when decreasing the particle size: $\theta = 240$ K, 220 K, 175 K, and 145 K for the A, B, C and D samples, respectively. The significance of this finding is at present unclear. However, it may be speculated that θ measures the strength of intergranular magnetic coupling; in that case, it is not inconceivable that as the particle size is reduced the magnetic interaction with neighbouring grains is more prominent.

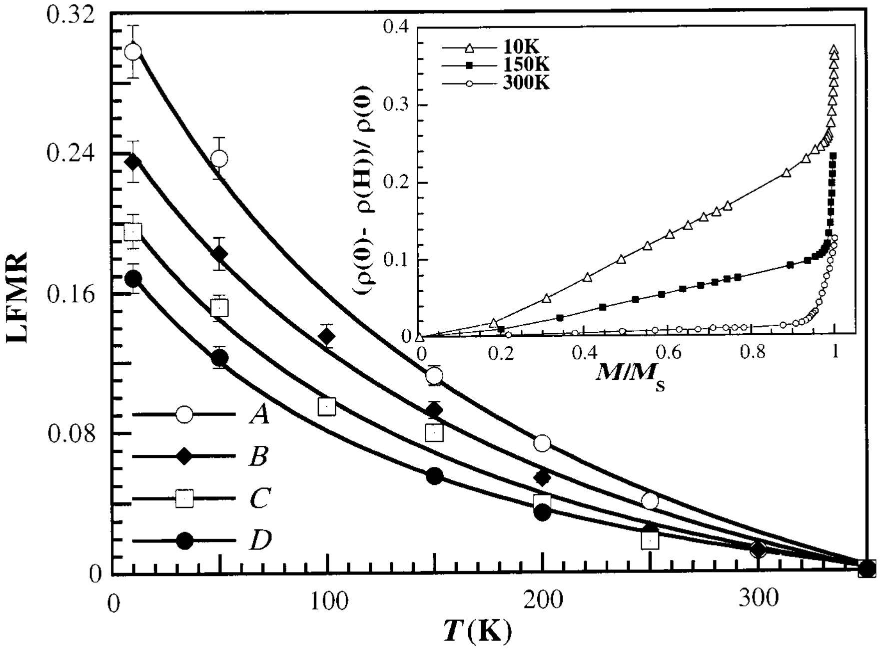

Figure 2. Low-field magnetoresistance as defined in the text versus temperature as a function of the particle size (0.5–1 μm (A), 2–5 μm (B), 10–20 μm (C) and 50–100 μm (D)). Inset: MR versus normalized magnetization; the absence of a quadratic dependence on M/M_s is evident.

On the other hand, the isothermal field dependence of the magnetization in ferromagnets can be described in terms of the so-called 'law of approximation to saturation' (LAS):

$$M(H) = M_\mathrm{s}[1 - a/H - b/H^2] + \chi_\mathrm{d} H, \tag{2.1}$$

where M_s is the saturation magnetization and $\chi_\mathrm{d} H$ is the high-field differential susceptibility and a, b are fitting parameters. In order to get an estimate of the magnetic anisotropy energy in these samples, we assume, to a first approximation, the expression of K_1 for uniaxial systems:

$$K_1 = [(105/8)bM_\mathrm{s}^2]^{1/2}. \tag{2.2}$$

The values obtained for K_1 are around 10^6 erg cm^{-3}. These values of the magnetic anisotropy are surprisingly large for a transition metal oxide. Nevertheless, they should be considered just as an upper limit for the magnetic anisotropy since, at the maximum field applied (55 kOe), samples may be far from saturation and other contributions (canting, frustration, etc.) may affect the values determined in this way. In any case, it is evident that decreasing the particle size implies an increment of the magnetic hardness that is reflected in the increase of the LFMR. Whether the origin of this hardness is an increase in the surface anisotropy or an increase in the magnetic frustration is still an open question. We think that it may be closely related to the existence of a magnetically disordered surface layer, as already observed in magnetic nanoparticles (Kodama *et al.* 1996), whose contribution increases as particle size decreases and is specially relevant for transport experiments since electrons have to cross through this surface layer from one grain to another.

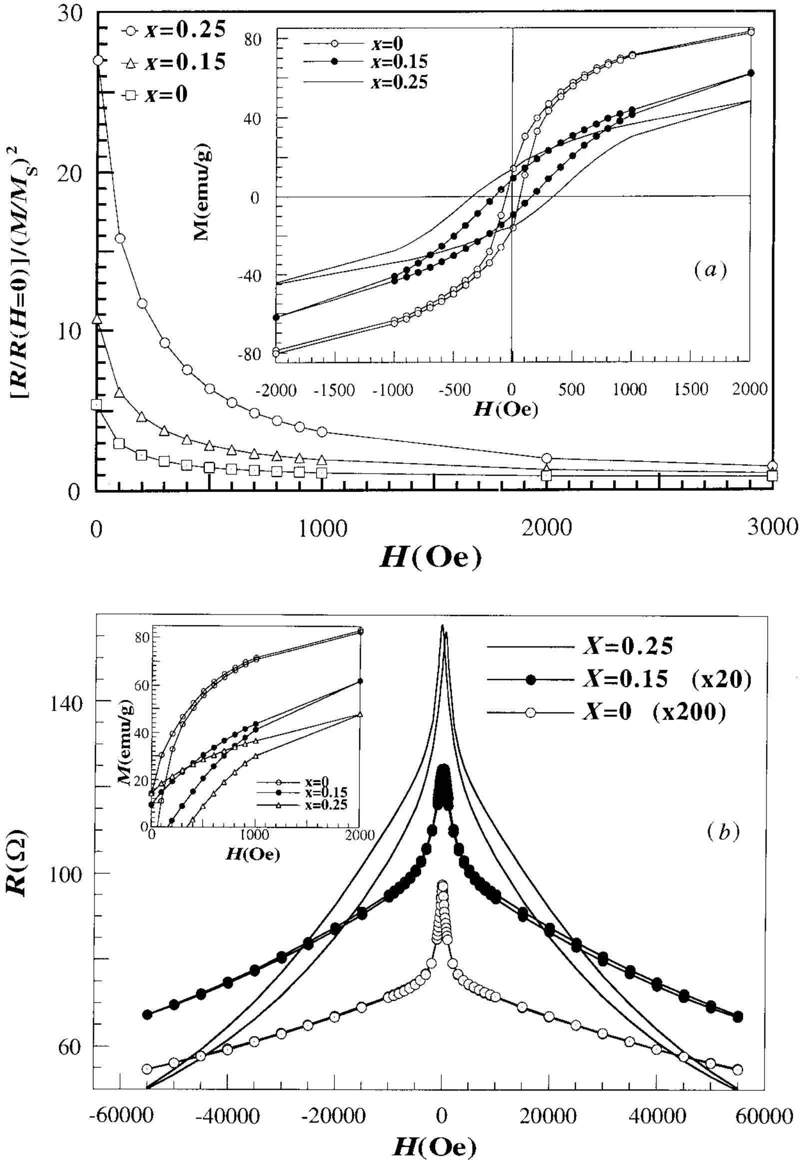

Figure 3. (*a*) Field dependence of the magnetoresistance $\rho(H)/\rho(H=0)$ normalized by reduced magnetization $(M/M_s)^2$. Inset: hysteresis loops of the magnetization $M(H)$. (*b*) Hysteresis loop of the resistivity $\rho(H)$ for the $x = 0$, 0.15, and 0.25 samples at 5 K. Inset: First quadrant of the magnetic loops.

In order to explore this idea further, it would be desirable to control the width of this disordered surface layer. To that purpose we have modified the strength of the ferromagnetic interaction, and thus the magnetic structure of the surface spins, by using ceramic samples of $La_{2/3-x}Y_xCa_{1/3}MnO_3$ (x = 0–0.25), with essentially the same particle size (*ca.* 1 µm). To reinforce the experimental evidence of surface modifications it is convenient to use small particles with a large specific surface.

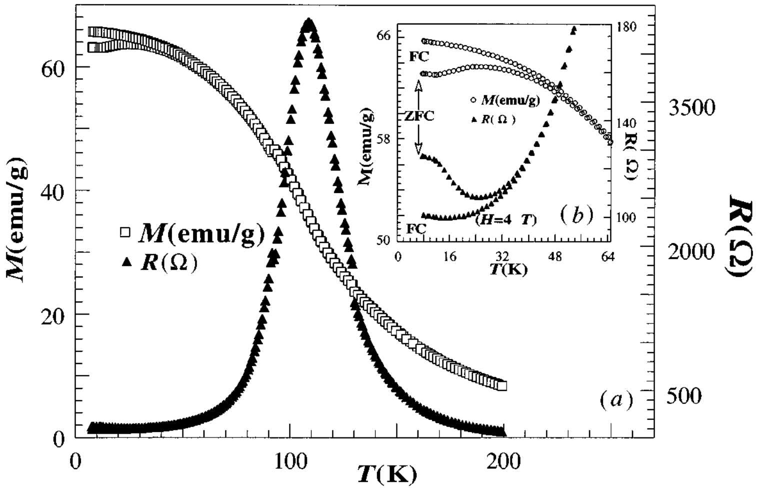

Figure 4. Magnetization $M(T)$ (a) and resistivity $\rho(T)$ (b) ZFC and FC curves measured at high fields ($H = 40$ kOe $\gg H_\mathrm{a}$) for $x = 0.25$. Inset: Zoom of the low temperature part.

For this the reason we have used in this part of the work samples prepared by sol-gel (Fontcuberta *et al.* 1998; Suzuki & Jardim 1996). As already mentioned in § 1, the competition between F and AF interactions can be tuned via the $\sigma^{1-x}(e_g)$ bandwidth. It is expected that when the F interactions are reduced the non-collinear surface layer becomes broader.

The Curie temperature, T_C, of the $x = 0$, 0.15, 0.25 samples, as determined from the position of the maximum in $\rho(T)$ measurements are 270 K, 114 K, and 88 K, whereas the corresponding tolerance factors are 0.897, 0.890, and 0.885, respectively. The $\rho(H)$ and $M(H)$ loops for samples with $x = 0$, 0.15, 0.25 at 5 K are shown in figure 3. It is found that both coercive fields, H_c, and anisotropy fields, H_a (less than 3 kOe) increase gradually with x showing no other contributions to the irreversibility than those coming from domain rotation.

Nevertheless, ZFC-FC measurements at high fields do show irreversible behaviour below about 40 K (see figure 4) and, as expected, the irreversibility becomes broader as x increases (not shown). The existence of magnetic irreversibility at such high fields (up to 55 kOe for $x = 0.25$) is attributed to the freezing of a part of the spin system into a metastable spin-glass-like state, in close similarity with what is observed in magnetic nanoparticles (Kodama *et al.* 1996).

As shown in figure 3b, the electrical resistivities display strongly enhanced hysteresis as compared to the magnetization and it is more evident as x increases. Notice, for instance, that for $x = 0.25$, at 5 K, $\rho(H)$ is irreversible up to 55 kOe, whereas $M(H)$ is closed at about 2 kOe.

In short, irreversibility in the resistivity appears to be more prominent than in the magnetization. This observation is extremely significant because it clearly shows that, even if a small fraction of the spins are frozen in a disordered configuration (the $M(H)$ loops are closed), the resistivity is still hysteretic. The most plausible explanation of this remarkable result is that electrical resistivity measurements sense the surface spin state at the grain boundaries. It is thus clear that any effect modifying the surface magnetization should change $\Delta\rho$. Therefore, the irreversibility in $\rho(T, H)$

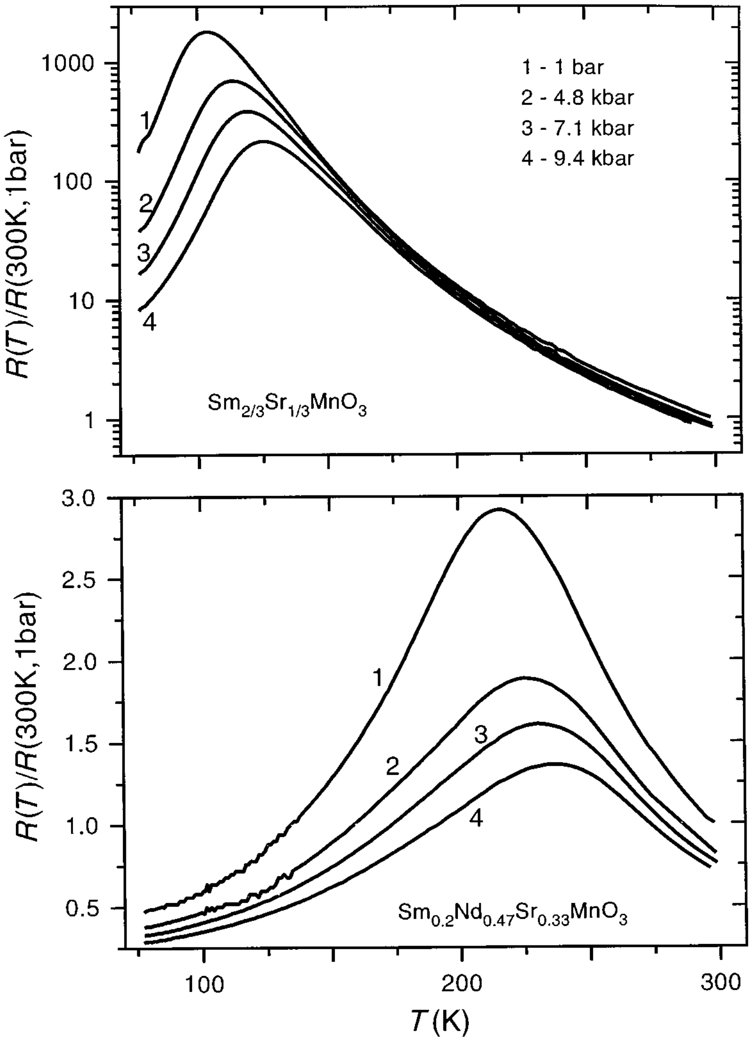

Figure 5. Normalized resistance versus temperature at several pressures for $Sm_{2/3}Sr_{1/3}MnO_3$ and $Sm_{0.2}Nd_{0.47}Sr_{1/3}MnO_3$ samples. The pressure labelling refers to the nominal pressure at room temperature.

reveals a quenched surface spin disorder. It also means that the surface glassiness displays significant magnetoresistance. It is clear that in our micrometric particles, the surface spin contribution to the magnetization should necessarily be only a minor fraction of the bulk magnetization. For instance, from the $\Delta M(10\,\mathrm{K}, 5\,\mathrm{kOe})$ value, one can estimate a non-magnetic layer of about 10 nm, that is only of about 1% of the particle radius.

Within the tunnelling-of-polarized-electrons model the magnetoresistance, $\Delta\rho$, is given by $\rho(H) \sim (J/T)M^2(T,H)$, where J is the intergrain exchange interaction (Helman & Abeles 1976). It is thus clear that any effect modifying the surface magnetization (and/or J) should change $\Delta\rho$. Significantly, as shown in the main panel of figure 3a, the interface magnetoresistance, typically observed in the low-field region, becomes more pronounced for samples having a narrower bandwidth. In this figure, the isothermal (5 K) field-dependent resistivity $\rho(H)/\rho(H = 0)$ normalized by the expected $(M/M_\mathrm{s})^2$ dependence has been plotted for all samples. For simplicity only the field-decreasing branches are depicted. A progressive enhancement of the low-field magnetoresistance is observed as the AF/F competition is reinforced (increasing the Y contents) and thus the effective interface broadens.

The resistivity measured after ZFC-FC processes also displays low-temperature hysteretic behaviour and, as expected, the FC resistivity is always lower than the ZFC one. In figure 4 we include the $\rho(T, 50\,\mathrm{kOe})$ data for the $x = 0.25$ sample. We note again the more pronounced irreversible character $\rho(T)$ when compared to $M(T)$: i.e. for $x = 0.25$, the difference in $\rho(T)$ (ZFC/FC) is of about 20% while $\Delta M =$ 3%. Therefore, the available experimental data, particularly the observation of open hysteresis loops, $\rho(H)$, up to fields well above (at least one order of magnitude) H_a can be well understood as a result of the existence of a significant spin disorder at the grain boundaries. The persistence of hysteresis on the resistivity when magnetization loops are almost reversible is a key observation which, essentially, reveals the surface nature of the spin disorder. This hysteresis is more pronounced in the Y-rich samples, an effect that is consistent with an enhanced magnetic frustration and the softer interatomic magnetic coupling (Fontcuberta *et al.* 1996*a*, *b*; Hwang *et al.* 1995*a*; Tokura *et al.* 1996). The observation of higher coercive fields for $x = 0.25$ than for $x = 0$ (figure 3) also fits into this picture.

In summary, we have shown that the MR of ceramic samples displays a clear dependence on the particle size, especially in the low-field regime. The magnetic behaviour shows that the system becomes magnetically harder as the particle size decreases. Whether this is due to an increase in magnetic surface anisotropy or an increase in the magnetic frustration is still an open question. However, it seems that spin disorder increases at grain surfaces. Low-field magnetoresistance could thus originate from the field-suppressed magnetic disorder at the particle surface layer. The relevance of these observations for the spin-polarized devices, where magnetic and electrical interfaces are at the heart, is thus clear, as polarization can be seriously reduced.

3. Pressure effects

Figure 5 shows, as typical examples, the temperature dependence of the normalized resistance $R(T)/R(300\,\mathrm{K}, 1\ \mathrm{bar})$ for $\mathrm{Sm_{2/3}Sr_{1/3}MnO_3}$ and $\mathrm{Sm_{0.2}Nd_{0.47}Sr_{1/3}MnO_3}$ samples at several pressures. It can be observed that a well-developed maximum of resistance appears at T_C. As expected, the application of pressure shifts T_C towards a higher temperature ($\mathrm{d}T_\mathrm{C}/\mathrm{d}P$ is *positive*); thus it stabilizes the metallic phase.

In figure 6 we show the normalized $T_\mathrm{C}(P)/T_\mathrm{C}(1\ \mathrm{bar})$ for some of the measured samples. When constructing this plot, the corrected value of P at the temperature where T_C occurs has been used. The slope $\mathrm{d}T_\mathrm{C}/\mathrm{d}P$ determined from the high-pressure portion of $T_\mathrm{C}(P)$ will be used from now as a convenient criterion for the sensitivity of T_C to pressure for all samples. This plot immediately reveals that, at a nominally constant hole density, the samples having higher T_C, i.e. larger R_o values and thus broader bandwidth W, are less sensitive to pressure than those of narrower bandwidth (that is lower T_C). In figure 7*a*, where we collect the slopes, $\mathrm{d}T_\mathrm{C}/\mathrm{d}P$, as a function of T_C ($P = 1$ bar), the saturating behaviour of $\mathrm{d}T_\mathrm{C}/\mathrm{d}P$ when lowering T_C

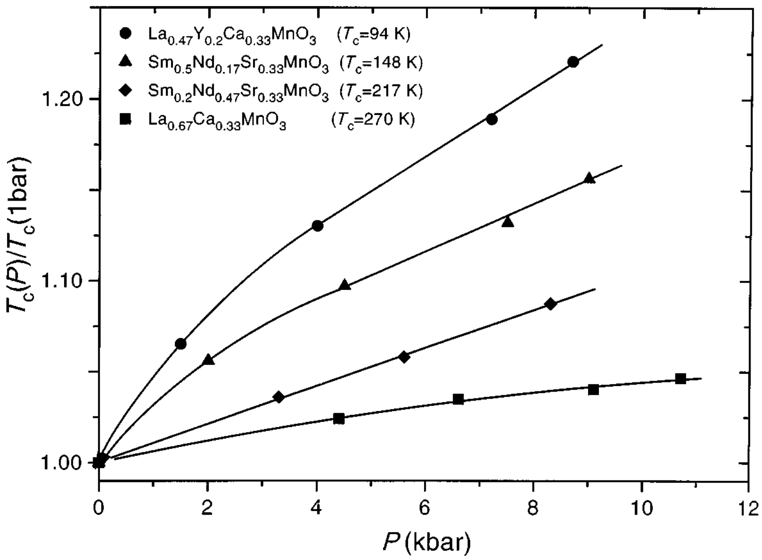

Figure 6. Pressure dependence of the normalized $T_C(P)/T_C(P = 1\text{ bar})$ for some samples. Curves are labelled by the corresponding $T_C(P = 1\text{ bar})$: $La_{2/3}Ca_{1/3}MnO_3$ (270 K), $Sm_{0.2}Nd_{0.47}Sr_{1/3}MnO_3$ (217 K); $Sm_{0.5}Nd_{0.17}Sr_{1/3}MnO_3$ (148 K); $La_{0.47}Y_{0.2}Ca_{1/3}MnO_3$ (94 K).

is apparent. The previously reported data for $La_{2/3}Ca_{1/3}MnO_3$ (Hwang *et al.* 1995*b*), and $La_{2/3}Sr_{1/3}MnO_3$ (Neumeier *et al.* 1995; Moritomo *et al.* 1995) agree well with the present results.

It will prove to be more illuminating to observe the variations of $\mathrm{d}\ln T_C/\mathrm{d}P$ as a function of T_C, as included in figure 7*b*. It turns out that $\mathrm{d}\ln T_C/\mathrm{d}P$ is almost linear with T_C (slope $\beta_{\text{exp}} \approx -1 \times 10^{-4}\ \text{kbar}^{-1}\ \text{K}^{-1}$).

In order to explore this result in detail we proceed as follows. Let us assume that the dependencies of W on the structural parameters $(d_{\text{Mn–O}}, \Theta)$ can be factorized: $T_C \sim W \sim f(d_{\text{Mn–O}})g(\Theta)$. Therefore,

$$\frac{1}{T_C}\frac{\mathrm{d}T_C}{\mathrm{d}P} = \frac{1}{f(d_{\text{Mn–O}})}\frac{\partial f(d_{\text{Mn–O}})}{\partial P} + \frac{1}{g(\Theta)}\frac{\partial g(\Theta)}{\partial P}. \tag{3.1}$$

Based on rather general principles, it can be shown that $f(d) \sim d^{-n}$ with $n \approx 7/2$ for the perovskite array (Harrison 1980). Therefore, the first term of the right-hand side of equation (3.1) simply reads $-n\kappa(d)$, where $\kappa(d)$ is the bond length compressibility. The angular dependence of the bandwidth $g(\Theta)$ can be written, to first order, as $g(\Theta) \sim \cos^2(\Theta)$ (Harrison 1980). Therefore, the second term of the right-hand side can be rewritten as $-2\tan(\Theta)\Theta(\kappa)$, where $\kappa(\Theta)$ is the bond angle compressibility. Therefore, equation (3.1) is transformed to

$$\frac{1}{T_C}\frac{\mathrm{d}T_C}{\mathrm{d}P} = -n\kappa(d) - 2\tan(\Theta)\Theta\kappa(\Theta), \tag{3.2}$$

which explicitly reveals the observed angular dependence of $(1/T_C)\mathrm{d}T_C/\mathrm{d}P$.

In order to evaluate equation (3.2), the reported bond compressibilities $(\kappa(d), \kappa(\Theta))$ for the $LNiO_3$ series can be taken as a reasonable starting point. Medarde *et al.* (1995) reported for $PrNiO_3$ at room temperature: $\kappa(d) = -4.38 \times 10^{-4}\ \text{kbar}^{-1}$ and $\kappa(\Theta) = 6.7 \times 10^{-4}\ \text{kbar}^{-1}$. According to available structural data for $L_{2/3}A_{1/3}MnO_3$

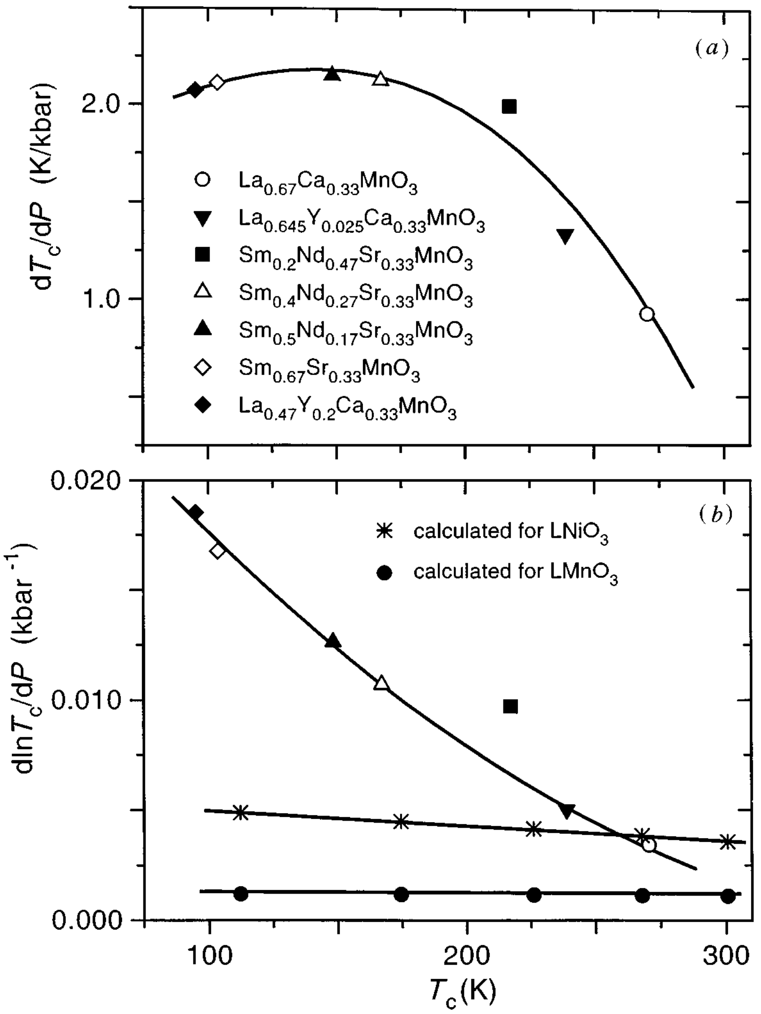

Figure 7. (*a*) Dependence of $\mathrm{d}T_\mathrm{C}/\mathrm{d}P$ on T_C. (*b*) Measured and calculated (using $\kappa(\Theta)$ and $\kappa(d)$ data for $\mathrm{LNiO_3}$ (stars) and $\mathrm{LMnO_3}$ (solid circles)) dependencies of the logarithmic slope $\mathrm{d}\ln T_\mathrm{C}/\mathrm{d}P$ on T_C.

oxides and for the range of R_o explored in this paper, Θ is in the 155–170° range (García-Muñoz *et al.* 1996*a*, 1997). Therefore, $(1/T_\mathrm{C})\mathrm{d}T_\mathrm{C}/\mathrm{d}P$ can be computed by using equation (3.2). It follows that both the bond length and the angular terms in equation (3.2) lead to positive contributions (that is both increase T_C under pressure) and are of the same order of magnitude. For instance, for $\Theta = 160°$, it turns out that

$$\frac{1}{f(d)}\frac{\partial f(d)}{\partial P} \approx 1.5\times10^{-3}\,\mathrm{kbar}^{-1} \quad \text{and} \quad \frac{1}{g(\Theta)}\frac{\partial g(\Theta)}{\partial P} \approx 1.4\times10^{-3}\,\mathrm{kbar}^{-1}.$$

It is thus clear that our estimate gives the correct sign for the overall $(1/T_\mathrm{C})\mathrm{d}T_\mathrm{C}/\mathrm{d}P$. In addition, equation (3.2) reveals one of the main results of the paper, that is when reducing Θ (or equivalently R_o) the relative variation of T_C under pressure increases. However, the quantitative agreement for the narrow band materials (low

Θ and T_C) is very poor: $(1/T_C)\mathrm{d}T_C/\mathrm{d}P$ is about one order of magnitude smaller than experimentally observed (see figure 7*b*). The comparison is favourable for the broader band materials (larger Θ).

In order to reach an improved estimate of the observed dependence of $(1/T_C) \times \mathrm{d}T_C/\mathrm{d}P$ on T_C, equation (3.1) should be computed for each T_C. This has been worked out in Laukhin *et al.* (1997). In figure 7*b* we show the results calculated (stars), i.e. $(1/T_C)\mathrm{d}\ln T_C/\mathrm{d}P$ versus T_C for LNiO$_3$. In the investigated range of variation of T_C, it is clear that $(1/T_C)\mathrm{d}T_C/\mathrm{d}P$ is linear with T_C as experimentally observed (see figure 7*b*).

Using the $\kappa(\Theta) \approx 1.6 \times 10^{-4}$ to 8.5×10^{-5} kbar^{-1} and $\kappa(d) \approx -2.32 \times 10^{-5}$ kbar^{-1} values reported recently by Radaelli *et al.* (1997) for $\mathrm{L}_{2/3}\mathrm{A}_{1/3}\mathrm{MnO}_3$ oxides, we have also computed $\mathrm{d}\ln T_C/\mathrm{d}P$ versus T_C for manganites. The results are included in figure 7*b* (solid circles). Due to the fact that $\kappa(\Theta)$ and $\kappa(d)$ are weaker than those reported for LNiO$_3$, the $\mathrm{d}\ln T_C/\mathrm{d}P$ values and the slope of $\mathrm{d}\ln T_C/\mathrm{d}P$ versus T_C, β_{theo} ($\approx 6 \times 10^{-7}$ kbar^{-1} K^{-1}) are correspondingly smaller. It is thus clear that the conclusions of our paper are unchanged. That is, bandwidth effects alone cannot account quantitatively for the observed $\mathrm{d}\ln T_C/\mathrm{d}P$ versus T_C variation.

The above derivation is based on the assumption that T_C is simply proportional to W and its variation by internal or external pressure is given by steric effects exclusively. Therefore, we should conclude that steric effects alone, modifying exclusively the bandwidth W cannot give an acceptable numerical estimate of the pressure effects on the insulator–metal transitions occurring at T_C in LMnO$_3$ oxides. Other alternatives should be explored.

It is clear that the above analysis overlooks the possibility that other bands are modified under pressure, or that the charge density in the bands is modified when varying the orbital overlapping. This situation is known to occur in superconducting cuprates (Gupta & Gupta 1991; García-Muñoz *et al.* 1996*b*) and in principle it could be expected to be present to a certain extent in these earlier transition metal oxides. Perhaps of more significance is the fact that the DE model ($T_C \sim W$) that we have used so far neglects the polaronic nature of charge carriers (Fontcuberta *et al.* 1996*b*; Zhao *et al.* 1996; de Teresa *et al.* 1997). Zhao *et al.* (1996) used the isotope effect to reveal the polaronic nature of carriers and they showed that

$$T_C \sim W \exp(-\gamma E_{\mathrm{JT}}/h\omega), \tag{3.3}$$

where E_{JT} is the Jahn–Teller energy, ω is an appropriate optical mode frequency and $0 < \gamma < 1$ is a parameter which itself depends on $E_{\mathrm{JT}}/h\omega$. Therefore, if equation (3.3) is used in combination with the measured isotope exponent ($\alpha = \frac{1}{2}\gamma E_{\mathrm{JT}}/h\omega$), it turns out that

$$\frac{\mathrm{d}\ln T_C}{\mathrm{d}P} = \frac{\mathrm{d}\ln W}{\mathrm{d}P} - 2\frac{\mathrm{d}\alpha}{\mathrm{d}P}. \tag{3.4}$$

According to data in Zhao *et al.* (1996), we note that $\mathrm{d}\alpha/\mathrm{d}P$ is negative, i.e. the phonon carrier coupling (given by α) becomes progressively weaker when broadening the bandwidth, that is increasing pressure. Therefore, it follows from equation (3.4) that the $\mathrm{d}\alpha/\mathrm{d}P$ term leads to a positive contribution to $\mathrm{d}\ln T_C/\mathrm{d}P$ that adds to the pure steric contribution given by $\mathrm{d}\ln W/\mathrm{d}P$. By using the $\alpha(R_o)$ data of Zhao *et al.* (1996) and the $\kappa(\Theta)$ values of Medarde *et al.* (1995), it turns out that $\mathrm{d}\alpha/\mathrm{d}P \approx -(0.01\text{–}0.02)$ kbar^{-1}.

It is encouraging to observe that when including the explicit dependence of the electron–phonon coupling on pressure in $\mathrm{d}\ln T_C/\mathrm{d}P$, i.e. the polaronic nature of the carriers, the evaluated pressure dependence of the Curie temperature turns out to be of the right order of magnitude and in a fairly good agreement with experimental data.

Consequently, our experimental data indicate that, contrary to what is usually accepted, steric effects do not, alone, account for the observed variation of T_C, either when applying internal or external pressure. Rearrangement of the electronic system and modifications of the electron–phonon coupling also appear to occur, leading to an additional contribution to $\mathrm{d}T_C/\mathrm{d}P$. A similar conclusion can be derived from the analysis of the pressure dependence of the resistivity in the paramagnetic state (Neumeier *et al*. 1995; Laukhin *et al*. 1998). Thermopower data under pressure (Zhou *et al*. 1996) also point in this direction.

In summary, we have shown that the pressure dependence of T_C of the metal–insulator transitions occurring in manganese perovskites, $\mathrm{d}\ln T_C/\mathrm{d}P$, becomes more pronounced when the relevant bandwidth becomes narrower. We have shown that this effect results from the particular dependence of the bandwidth on the M–O–M bond angle and its compressibility under pressure. We have also demonstrated that steric effects on the bandwidth are not enough to account for the measured $\mathrm{d}\ln T_C/\mathrm{d}P$ variations and other effects, presumably related to polaronic nature of carriers, have to be considered. In particular, our data strongly suggest that the electron–phonon coupling is strong when reducing the bandwidth. These findings are of relevance for the understanding of the metal–insulator transitions observed in these perovskites. According to our analysis these conclusions are not only restricted to the manganese case but also to nickel perovskites, where substantial electron–phonon coupling is predicted. Isotope experiments on these latter compounds will be welcome as they can definitively settle this question.

We acknowledge the CiCYT (MAT97-0699 and MAT94-1924), the GRQ-95-8029 and the OXSEN-CEE Projects for financial support. V.L. is grateful to NATO for a grant.

References

Balcells, Ll., Fontcuberta, J., Martínez, B. & Obradors, X. 1998 *J. Phys.* C **10**, 1883.

de Teresa, J. M., Ibarra, M. R., García, J., Blasco, M., Ritter, C., Algarabel, P. A., Marquina, C., del Moral, A. & Arnold, Z. 1997 *Nature* **386**, 256.

Fontcuberta, J., Martínez, B., Seffar, A., Piñol, S., García-Muñoz, J. L. & Obradors, X. 1996*a* *Phys. Rev. Lett.* **76**, 1122.

Fontcuberta, J., Martínez, B., Seffar, A., Piñol, S., García-Muñoz, J. L. & Obradors, X. 1996*b* *Europhys. Lett.* **34**, 379.

Fontcuberta, J., Martínez, B., Balcells, Ll., Obradors, X., Cohenca, C. H. & Jardim, R. F. 1998 *J. Appl. Phys.* **83**. (In the press.)

García-Muñoz, J. L., Fontcuberta, J., Suaaidi, M. & Obradors, X. 1996*a* *J. Phys. Condensed Matter* **8**, L787.

García-Muñoz, J. L., Suaaidi, M., Fontcuberta, J., Piñol, S. & Obradors, X. 1996*b* *Physica* C **268**, 173.

García-Muñoz, J. L., Fontcuberta, J., Martínez, B., Seffar, A., Piñol, S. & Obradors, X. 1997 *Phys. Rev.* B **55**, R668.

Gupta, R. P. & Gupta, M. 1991 *Physica* C **173**, 357.

Harrison, W. 1980. In *Electronic sructure and properties of solids.* San Francisco: Freeman.

Helman, J. S. & Abeles, B. 1976 *Phys. Rev. Lett.* **37**, 1429.

Hwang, H. Y., Cheong, S.-W., Radaelli, P. G., Marezio, M. & Batlogg, B. 1995*a* *Phys. Rev. Lett.* **75**, 914.

Hwang, H. Y., Plastra, T. T. M., Cheong, S.-W. & Batlogg, B. 1995*b* *Phys. Rev.* B **52**, 15046.

Hwang, H. Y., Cheong, S.-W., Ong, N. P. & Batlogg, B. 1996 *Phys. Rev. Lett.* **77**, 2041.

Jin, S., Tiefel, T. H., McCormack, M., Fastnacht, R. A., Ramesh, R. & Chen, L. H. 1994 *Science* **264**, 463.

Kodama, R. H., Berkowitz, A. E., McNiff Jr, E. J. & Foner, S. 1996 *Phys. Rev. Lett.* **77**, 394.

Laukhin, V., Fontcuberta, J., García-Muñoz, J. L. & Obradors, X. 1997 *Phys. Rev.* B **56**, R10 009.

Laukhin, V., *et al.* 1998 (In preparation.)

Li, X. W., Gupta, A., Gang Xiao & Gong, G. Q. 1997 *Appl. Phys. Lett.* **71**, 1124.

Medarde, M., Mesot, J., Lacorre, P., Rosenkranz, S., Fisher, P. & Gobrecht, K. 1995 *Phys. Rev.* B **52**, 9248.

Moritomo, Y., Asamitsu, A. & Tokura, Y. 1995 *Phys. Rev.* B **51**, 16491.

Neumeier, J. J., Hundley, M. F., Thompson, J. D. & Heffner, R. H. 1995 *Phys. Rev.* B **52**, R7006.

Radaelli, P. G., Iannon, G., Marezio, M., Hwang, H. Y., Cheong, S.-W., Jorgensen, J. D. & Argyriou, D. N. 1997 *Phys. Rev.* B **56**, 8265.

Suzuki, P. A. & Jardim, R. 1996 *Physica* C **267**, 153.

Tokura, Y., Tomioka, Y., Kuwahara, H., Asamitsu, A., Moritomo, Y. & Kasai, M. 1996 *Phys. Rev. Lett.* **76**, 3184.

Zhao, G., Conder, K., Keller, H. & Muller, K. A. 1996 *Nature* **381**, 676.

Zhou, J.-S., Archibald, W. & Goodenough, J. B. 1996 *Nature* **381**, 770.

Discussion

T. T. M. Palstra (*University of Groningen, The Netherlands*). Could Dr Fontcuberta comment on the source of the surface anisotropy. In other papers in this volume, we learn that only nearest-neighbour interactions are important, so it is difficult to understand the large degree of magnetic disorder on the surface.

J. Fontcuberta. First, one should expect that the ferromagnetic order close to the surface in these double-exchange materials is going to be strongly suppressed because carrier mobility should be dampened and so ferromagnetic coupling is going to be weaker. Consequently, competition with the antiferromagnetic background is expected to be reinforced, eventually leading to some frustration.

Secondly, the origin of the magnetic anisotropy is a subject of strong discussion in nanoparticle magnetic systems. What I can simply say here is that it becomes harder to orient the spins close to the surface; this is an experimental result well established in nanoparticle systems. However, the origin of this anisotropy—why it becomes harder to orient the spins—is not well settled.

A. J. Millis (*The Johns Hopkins University, USA*). First, regarding Tom Palstra's question, many measurements tell us that the surface is very non-trivial: measurements on thin films tell you that there is a magnetic dead layer of a number of angstroms, etc. Just from the point of view of local chemistry, the surface is very different from the bulk and so it's not surprising that it is different. I guess one should be very careful about trying to guess from bulk measurements how the surface is likely to behave; there is obviously major reconstruction.

To come back to the pressure dependence, how do Dr Fontcuberta's data agree with those published by Moritomo *et al*. (1995), who looked at the pressure dependence of T_C in a wide range of pressures?

J. Fontcuberta. Mortimo *et al*. (1995) reported data on samples having different doping levels, so results cannot be directly compared. However, these authors reported values of $\mathrm{d}\ln T_C/\mathrm{d}P$ very similar to ours for their $La_{2/3}Sr_{1/3}MnO_3$ sample. Now, we are preparing a review including 'all' $\mathrm{d}\ln T_C/\mathrm{d}P$ data for $x = 1/3$ from the literature (Fontcuberta *et al*. 1998). The results are fully consistent with our present data: i.e. $\mathrm{d}\ln T_C/\mathrm{d}P$ becomes larger when reducing T_C. What we have provided here is an explanation for this huge effect, which becomes more prominent as the bandwidth is reduced (T_C lowered), and which cannot be accounted for by simple consideration of steric effects. It results from a more intense electron–phonon coupling when the bandwidth is narrowed.

A. J. Millis. We know that in one material, and my guess is that it is true in general, the sensitivity to volume-preserving strain is likely to be much greater than the sensitivity to hydrostatic pressure. So the effects Dr Fontcuberta found are big, but my guess is that there are much bigger effects waiting for a volume-preserving measurement (for $La_{0.83}Sr_{0.17}MnO_3$ this has been shown in Millis *et al*. (1998)).

J. R. Cooper (*University of Cambridge, UK*). Could I clarify that it is going in the right direction, because in my experience when you apply a pressure all the polaron effects and strain effects generally get weaker. This is certainly the case in organic conductors, for example. So, are the polaron effects getting bigger or smaller under pressure?

J. Fontcuberta. Smaller, as you would expect.

Additional references

Fontcuberta, J., Laukhin, V. & Obradors, X. 1998 *Appl. Phys. Lett.* **72**, 2607.
Millis, A. J., Darling, T. & Migliori, A. 1998 *J. Appl. Phys.* **83**, 1588.